Autism spectrum disorder susceptibility gene TAOK2 affects basal dendrite formation in the neocortex

Citation: Calderon de Anda, Froylan, Ana Lucia Rosario, Omer Durak, Tracy Tran, Johannes Gräff, Konstantinos Meletis, Damien Rei, et al. "Autism Spectrum Disorder Susceptibility Gene TAOK2 Affects Basal Dendrite Formation in the Neocortex." Nat Neurosci 15, no. 7 (June 10, 2012): 1022–1031.

As Published: http://dx.doi.org/10.1038/nn.3141

Publisher: Nature Publishing Group

Persistent URL: http://hdl.handle.net/1721.1/92919

Version: Author's final manuscript: final author's manuscript post peer review, without publisher's formatting or copy editing

Published in final edited form as:
Nat Neurosci. ; 15(7): 1022–1031. doi:10.1038/nn.3141.

An Autism Spectrum Disorder Susceptibility Gene, TAO2, is Important for Basal Dendrite Formation in the Neocortex

Froylan Calderon de Anda[1,2], **Ana Lucia Rosario**[1,2], **Omer Durak**[1,2,3], **Tracy Tran**[2,4,6], **Johannes Gräff**[1,2], **Konstantinos Meletis**[1,2,3,7], **Damien Rei**[1,2], **Takahiro Soda**[1,2], **Ram Madabhushi**[1,2], **David D. Ginty**[2,4], **Alex L. Kolodkin**[2,4], and **Li-Huei Tsai**[1,2,3,5]

[1]Department of Brain and Cognitive Sciences, Picower Institute for Learning and Memory, Massachusetts Institute of Technology, 77 Massachusetts Avenue, Building 46, Room 4235A, Cambridge, MA 02139, U.S.A.

[2]Howard Hughes Medical Institute, 77 Massachusetts Avenue, Building 46, Room 4235A, Cambridge, MA 02139, U.S.A.

[3]Stanley Center for Psychiatric Research, Broad Institute, Cambridge, MA 02139, U.S.A.

[4]Solomon H. Snyder Department of Neuroscience, The Johns Hopkins University School of Medicine, Baltimore, Maryland 21205, U.S.A.

Abstract

How neurons develop their morphology is an important question in neurobiology. Here we describe a novel pathway that specifically affects the formation of basal dendrites and axonal projections in cortical pyramidal neurons. We report that thousand-and-one-amino acid 2 (TAO2) kinase plays an essential role in dendrite morphogenesis. TAO2 down-regulation impairs basal dendrite formation *in vivo* without affecting apical dendrites. Moreover, TAO2 interacts with Neuropilin 1 (Npn1), a receptor protein that binds the secreted guidance cue Semaphorin 3A (Sema3A). TAO2 over-expression restores dendrite formation in cultured cortical neurons from $Npn1^{Sema-}$ mice, which express Npn1 receptors incapable of binding Sema3A. TAO2 over-expression also ameliorates the basal dendrite impairment resulting from Npn1 down-regulation *in vivo*. Finally, Sema3A and TAO2 modulate the formation of basal dendrites through the activation of the c-Jun N-Terminal Kinase (JNK). These results delineate a pathway whereby Sema3A and Npn1 transduce signals through TAO2 and JNK to regulate basal dendrite development in cortical neurons.

[5]Correspondence: Li-Huei Tsai, lhtsai@mit.edu, (O): 617-324-1660, (F): 617-324-1657.
[6]Present address: School of Medicine, Rutgers University 225 University Ave. Life Science Center, Rm601D Newark NJ 07102 U.S.A.
[7]Present address: Department of Neuroscience, Karolinska Institutet, Retzius väg 8, S-17177 Stockholm, Sweden.

Author contributions.
This study was designed, directed, and coordinated by F.C.A. and L.-H.T. L.-H.T., as the principal investigator provided conceptual and technical guidance for all aspects of the project. F.C.A. planned and performed the *in utero* electroporations and analyzed the data with A.L.R. and O.D.; F.C.A. performed and analyzed the immunohistochemistry experiments. K.M. generated and characterized the shRNA constructs. K.M., A.L.R., and D.R. contributed to the neuronal cultures. T.T. performed and analyzed the data from the neuronal cultures of $Npn1^{Sema-}$ mice. A.L.R., O.D., J.G. and R.M. contributed to the biochemistry experiments. T.S. generated the lentiviral shRNA construct and produced the virus particles. D.D.G. and A.L.K. provided the $Npn1^{Sema-}$ mice brains and suggested and commented on the design of the experiments. The manuscript was written by F.C.A. and L.-H.T. and commented on by all authors.

Introduction

Pyramidal neurons are abundant in brain regions associated with complex cognitive functions, including the cortex, hippocampus, and the amygdala[1]. An understanding of the unique physiology and morphology of these neurons is key to the elucidation of the mechanisms underlying sophisticated cognitive functions in normal and disease conditions. Several lines of evidence suggest that aberrant dendritic arborization may contribute to neurodevelopmental and psychiatric disorders with delayed onset, such as autism spectrum disorders[2, 3]. In general, pyramidal neurons have a dendritic tree that is divided into two domains – the apical dendrite, which extends towards the pial surface, and basal dendrites, which emerge from the base of the cell body. The majority of synapses received by neocortical pyramidal neurons form on the basal dendrites[4]. However, little is known about the molecular pathways that control the formation of basal dendrites.

TAO1 and TAO2 serine/threonine protein kinases are known to activate mitogen-activated protein (MAP) kinase pathways (JNK, p38, or extracellular signal-regulated kinase[5, 6]), leading to the modulation of gene transcription. In humans, the gene encoding *TAO2*, a member of the MAP Kinase Kinase Kinase (MAPKKK) family, is located on chromosome 16p11.2, a region that has recently been shown to carry substantial susceptibility to autism spectrum disorders[7] and schizophrenia[8]. *TAO2* mRNA is also a direct target of the Fragile X protein, FMRP[9], whose loss or dysfunction leads to an autistic phenotype. TAO2 selectively activates mitogen-activated protein/ extracellular signal-regulated kinase kinases (MEKs)[10] and serves as a regulator of p38 MAPK. In addition, TAO2 modulates the actin cytoskeleton in non-neuronal cells through the activation of JNK[11]. TAO2 is subjected to alternative splicing to produce the TAO2α (140KD) and TAO2β (120KD) isoforms[12], of which only TAO2α stimulates the JNK pathway[13].

In the current report, we demonstrate that TAO2 down-regulation selectively impairs the formation of basal dendrites and axonal elongation. We found that TAO2 interacts with Npn1, the receptor of the secreted guidance cue Sema3A that controls basal dendrite arborization[14–17]. Sema3A induces TAO2 phosphorylation, thereby activating TAO2. In conditions in which Npn1 is either not expressed, or is not capable of binding Sema3A, basal dendrite formation deficits can be restored by TAO2 over-expression. TAO2 down-regulation also leads to JNK inactivation that manifests as a decrease of JNK phosphorylation in cultured cortical neurons. Over-expression of a constitutively active JNK1 (MKK7-JNK1) restores basal dendrite formation in cortical neurons following TAO2 down-regulation. Overall, these data support the role of a signaling axis involving Sema3A, Npn1, TAO2, and JNK1 in the regulation of basal dendrite formation in the developing cortex.

Results

Expression profile of TAO2 in cultured cortical neurons and in the developing cerebral cortex

To examine the subcellular expression profile of TAO2, we analyzed TAO2 immunoreactivity in 2 days *in vitro* (DIV) cultured cortical mouse neurons dissociated at embryonic day 17 (E17). We found that TAO2 preferentially localized to growth cones (Fig. 1a, b). The growth cone is a region where actin, but not microtubules, accumulates (Fig. 1b) and where the actin cytoskeleton is the most dynamic[18]. In contrast, TAO2 activated by phosphorylation on Ser 181 (pTAO2) localizes to the neurite shaft, where microtubules also accumulate (Fig. 1c). This pattern of TAO2 expression suggests that TAO2 may act as a coordinator of actin and microtubule dynamics[19].

In the mouse brain, TAO2 and pTAO2 are preferentially expressed in the intermediate zone (IZ) and the cortical plate (CP) of the developing cortex (E18), and their expression in the ventricular zone is low (VZ; Fig. 1d). Western blot analysis using whole-cell extracts from the cortices of mice at different embryonic and postnatal ages demonstrates that the long isoform of TAO2 (TAO2α; 140 KD) is expressed throughout early cortical embryonic development and increased in perinatal (E19, P0) and adult mice. In contrast, the short isoform of TAO2 (TAO2β; 120KD) was only observed perinatally and in the adult (Fig. 1e). In addition, in DIV2 E17 cortical neurons, we detected expression of TAO2α, but not TAO2β (data not shown). These results suggest that TAO2α is likely to be the TAO2 isoform most important for neuronal differentiation. We therefore focused our subsequent studies on TAO2α.

TAO2 impacts neuronal differentiation in cultured cortical neurons

The remodeling of the actin-based cytoskeleton is an important regulatory step in axon and dendrite formation[20–22]. Since it has been shown that TAO2 modulates the organization of the actin cytoskeleton in non-neuronal cells[11], and we found TAO2 expression to be concentrated in actin-rich structures, we asked whether TAO2 loss-of- and gain-of-function affects neuronal differentiation. For this, we designed three specific short-hairpin (sh)RNAs targeting different coding sequences of TAO2 to acutely knock down the expression of TAO2. We confirmed the specificity of our shRNA constructs with respect to their ability to down-regulate endogenous neuronal TAO2 in cortical neurons at E17 from embryos that had been transfected by *in utero* electroporation at E15 with constructs expressing TAO2 shRNA or control shRNA and membrane-bound GFP (F-GFP). Neurons were cultured for 48 h before being processed for immunocytochemistry using antibodies against TAO2 and acetylated tubulin (Fig. S1a–d; data not shown for shRNA 3). We also assessed the specificity of our shRNA constructs by western blot analysis in Ht22 cells (Fig. S1e, f; data not shown for shRNA 3). These experiments show that TAO2 shRNAs efficiently down-regulate TAO2 expression. shRNAs 1 and 2 were used for all subsequent experiments.

We first examined the impact of TAO2 knockdown on the cytoskeleton and growth cone morphology in primary neurons. We found that the shRNA-mediated knockdown of TAO2 decreased the F-actin content in the growth cones of cultured cortical neurons (Fig. 2a, b)

and the number of intact (non-collapsed) growth cones per neuron, compared with control-transfected neurons (Fig. 2a, c). In addition, TAO2 down-regulation decreased the number of neurites per neuron (Fig. 2a, d) and the number of secondary branches per cell (Fig. 2a, e). TAO2 autophosphorylation is known to play a role in TAO2 activation[10,13], thus the over-expression of TAO2 increased levels of phosphorylated, active TAO2 (Fig. S1g, h). TAO2 over-expression in cultured cortical neurons increased the number of primary, but not secondary, neurites compared with control neurons (Fig. 2a).

In addition, we analyzed whether TAO2 down-regulation or over-expression affects polarization in cultured neurons. We found that TAO2 down-regulation impaired axon formation (Fig. S2a). Interestingly, TAO2 over-expression did not affect the number of polarized (axon-bearing) neurons (Fig. S2a), but did increase the proportion of neurons that elaborated multiple axons (Fig. S2b, c). To determine if these phenotypes resulted specifically from the down-regulation of TAO2, we co-expressed TAO2 shRNA1 with a shRNA-resistant version of TAO2 cDNA (humanTAO2 cDNA, hTAO2), which rescued the TAO2 shRNA1 phenotypes. This molecular replacement experiment further demonstrated the specificity of TAO2 shRNA1 treatment (Fig. 2a–e and Fig. S2a).

Together, these data demonstrate that TAO2 is critical for the morphological differentiation of cultured cortical neurons.

TAO2 affects basal dendrite formation and axon elongation in vivo

We then sought to determine the effect of TAO2 in the post-migratory differentiation of cortical neurons *in vivo*. E15 mouse embryos were *in utero* electroporated with TAO2 shRNA, control shRNA, or ratTAO2 cDNA (rTAO2) plasmids together with F-GFP. Mice were sacrificed at postnatal day 7 (P7), and the dendritic morphology of control shRNA, TAO2 shRNA, and rTAO2-expressing neurons was evaluated. We found that both the knockdown and over-expression of TAO2 disrupted cortical neuronal differentiation *in vivo*. In layer II-III of the *in utero* electroporated brains, the TAO2 shRNA-transfected neurons had significantly fewer primary dendrites compared to controls (Fig. 3a, b). TAO2 over-expression, on the other hand, increased the number of primary dendrites (Fig. 3a, b). Sholl analysis of the dendritic arbors from shRNA-transfected neurons revealed that TAO2 down-regulation produced less complex basal dendritic arbors than control shRNA transfection. TAO2 shRNA-transfected neurons had significantly fewer dendritic processes with intersections at a distance between 15 μm and 55 μm from the cell soma (Fig. 3c). In contrast, TAO2 over-expression increased the complexity of the basal dendritic arbor compared to control-transfected neurons (Fig. 3c). Importantly, Sholl analysis demonstrated that TAO2 down-regulation or TAO2 over-expression did not affect the apical dendrites of transfected neurons (Fig. 3d; Fig. S3a).

To determine if the basal dendrite phenotype was exclusive to upper-layer neurons, or a more general feature of pyramidal neurons in the different cortical layers, we knocked-down TAO2 expression in deeper layer neurons (layer V) by *in utero* electroporating E13 embryos with TAO2 shRNA or control shRNA plasmids together with F-GFP. Animals were harvested at P4 to evaluate the dendritic morphology of transfected neurons in layer V. TAO2 down-regulation using either shRNA 1 or 2 also impaired the basal dendrite

complexity of layer V pyramidal neurons (Fig. S3b, c), without affecting apical dendrite complexity (Fig. S3d). These findings demonstrate that TAO2 loss-of- or gain-of-function impairs pyramidal neuron basal dendrite formation in the developing neocortex.

We also examined the contribution of TAO2 to axon elongation during brain development. We performed sequential *in utero* transfection as previously reported[23]. mCherry expression and control shRNA constructs were introduced into E15 mouse cortex, followed by the introduction of a TAO2 shRNA and Venus-expressing constructs into the contra-lateral hemisphere. Callosal axons from transfected neurons crossing into the midline were examined at P7. TAO2 down-regulation impaired axon elongation and axons were absent in the midline (Fig. 3e, f). On the other hand, TAO2 over-expression caused some transfected axons to deviate from the axonal tract (Fig. S3e). These results strongly support the role of TAO2 in axon elongation in the mouse *in vivo*, as was previously reported in *Drosophila*[19].

TAO2 interacts with the Neuropilin 1 receptor to modulate neuronal differentiation

Previous studies have shown that the Sema3A – Npn1/PlexinA4 signaling cascade controls basal dendritic arborization[14–16]. *Npn1*$^{Sema-}$ mice also develop axonal projection defects in the corpus callosum and the hippocampus[14]. These defects vary from mild phenotypes, in which some axons deviate from the axonal tract, to more severe ones, where callosal axons defasciculate and do not cross the midline[14]. We hypothesized that TAO2 may interact with this pathway to modulate neuronal differentiation. To test this idea, we performed co-immunoprecipitation experiments to probe for an interaction between TAO2 and Npn1. We co-expressed TAO2 and Npn1-mCherry in HEK293 cells and found that TAO2 interacts with Npn1-mCherry (Fig. 4a). To investigate whether this complex also forms *in vivo*, cortices from P0 mice were homogenized and subjected to co-immunoprecipitation using antibodies against Npn1 and TAO2. We found that Npn1 associates with TAO2 in lysates from P0 mouse cortices (Fig. 4b).

TAO2 is activated by phosphorylation on Ser 181, which resides in the activation loop of the kinase[24]. To determine whether Sema3A/Npn1 activates TAO2, we first examined whether active TAO2 co-localizes with Npn1. In the mouse E19 cerebral wall, we found that pTAO2 and Npn1 co-localized preferentially in the IZ and lower CP, where axons elongate and deeper layer neurons begin to form dendrites[25] (Fig. 4c, d).

Next, we examined whether the Npn1 ligand Sema3A modulates TAO2 phosphorylation in cultured primary neurons. Cortical neurons dissociated from E17 mouse embryos and cultured for 48 h were treated with Sema3A (2 μg/ml) for 30 min, 1 h, 2 h, or 6 h. pTAO2 immunoreactivity was significantly increased between 1 and 6 h following Sema3A treatment in the longest neurite analyzed (the putative axon, 40 μm < neurite length < 150 μm) compared to that of non-treated control cells (Fig. 4e, f). Western blot analysis of lysates harvested from neurons following 2 h of Sema3A treatment revealed that endogenous TAO2 phosphorylation was also induced following Sema3A treatment (Fig. 4g; Control = 1 ± 0.03, Sema3A = 1.32 ± 0.14-fold; n=3 experiments per duplicate; **P*=0.0401 by *t* test). Finally, we examined the levels of pTAO2 in cortical extracts from mice homozygous for a knock-in mutation that renders the endogenous Npn1 receptor incapable of binding Sema3A (*Npn1*$^{Sema-}$). In agreement with our *in vitro* experiments, we found that

pTAO2 levels are reduced in the cortical neurons of homozygous *Npn1*$^{Sema-}$ mice compared with heterozygous littermates (Fig. 4h; (+/−) = 1 ± 0.10, (−/−) = 0.56 ± 0.09-fold; n(+/−) = 9 brains, n(−/−) = 4 brains; **P*=0.0310 by *t* test). These results suggest that Sema3A signaling activates TAO2 kinase activity.

TAO2 and Sema3A modulate the activity of JNK in cortical neurons

We next sought to elucidate the downstream effectors by which the interaction of TAO2 with the Sema3A-Npn1 signaling pathway modulates neuronal differentiation in cortical pyramidal neurons. The JNK have been shown to be important for many aspects of neuronal differentiation[26]. It was shown that TAO2α, unlike TAO2β, stimulates the JNK pathway in cell lines[13]. TAO2 over-expression indirectly activates endogenous JNK1 in 293 cells via the preferential phosphorylation of MEK3 and MEK6[5]. In addition, TAO2 was shown to modulate the dual phosphorylation of JNK1 at Thr183/Tyr185[5, 27]. Sema3A has also been shown to activate the JNK1/c-Jun signaling pathway in cultured dorsal root ganglion neurons[28]. Phosphorylated JNK1/2 can modulate neurite initiation, axon formation, and dendritic architecture in cultured neurons[29–33] and is required for the maintenance of neuronal microtubules in axons and dendrites *in vivo*[34]. The deactivation of JNK1 by BDNF treatment destabilizes microtubules and induces axonal branching[35]. Based on these findings, we hypothesized that JNK1 may mediate the effect of TAO2 and Sema3A on neuronal differentiation.

To determine whether TAO2 modulates JNK1 in cortical neurons, we introduced TAO2 shRNA 1 or control plasmids together with F-GFP into E15 mouse embryos via *in utero* electroporation and isolated cortical neurons at E17. These neurons were cultured for 48 h before being subjected to immunocytochemistry using antibodies against phosphorylated JNK1 (pJNK; Thr-183/Tyr-185), which represents the active form of JNK1. TAO2 down-regulation decreased pJNK1 immunoreactivity in the longest neurite analyzed from shRNA-transfected neurons, compared to that from control-transfected neurons (Fig. 5a, b). Additionally, in Ht22 cells transfected with TAO2 shRNA 1, endogenous pJNK1 (top panel, lower band, 46 kD) was significantly reduced (Fig. 5c; Control = 1 ± 0.17, TAO2 shRNA 1 = 0.76 ± 0.09-fold, n=4 experiments per triplicate; **P*=0.0233 by *t* test).

As TAO2 interacts with Npn1, we asked whether treatment with the Npn1 ligand Sema3A modulates JNK1 phosphorylation in cultured primary neurons. Since JNK1 phosphorylation is enriched in developed axons[31], we used cultured neurons during the initiation of polarization to avoid endogenous JNK1 phosphorylation, which could mask that induced by our Sema3A treatment. Cortical neurons dissociated from E17 mouse embryos and cultured for 48 h were treated with Sema3A (2 μg/ml) for 30 min, 2 h, or 6 h. The levels of pJNK1 were measured using immunocytochemistry and western blot analysis. pJNK1 immunoreactivity was significantly increased at 2 h and 6 h following Sema3A treatment in the longest neurite analyzed (the putative axon, 40 μm < neurite length < 150 μm) compared to that in non-treated control cells (Fig. 5d, e). Western blot analysis of lysates harvested from neurons following 6 h of Sema3A treatment revealed that endogenous JNK1 phosphorylation (pJNK, top panel, lower band, 46 kD) was also induced following Sema3A treatment (Fig. 5f, Control = 1 ± 0.06, Sema3A = 1.59 ± 0.19-fold; n=3 experiments per

duplicate; **P=0.0014 by t test). We also examined the levels of pJNK1 in cortical extracts from $Npn1^{Sema-}$ mice. In agreement with our *in vitro* experiments, we found that pJNK1 levels were reduced in the cortical neurons of homozygous $Npn1^{Sema-}$ mice compared with heterozygous littermates (Fig. 5g; (+/−) = 1 ± 0.11, (−/−) = 0.54 ± 0.13-fold; n(+/−) = 9 brains, n(−/−) = 4 brains; *P=0.0382 by t test).

Sema3A and TAO2 may modulate JNK1 via a common mechanism; alternatively, they may regulate JNK1 via distinct pathways. To differentiate between these possibilities, we evaluated JNK1 activation following Sema3A treatment in the absence or presence of TAO2. Primary neurons were infected with recombinant lentivirus carrying control or TAO2 shRNA 1 soon after plating. Three days later, we assessed levels of pJNK1 following the addition of exogenous Sema3A (2 μg/ml). Sema3A increased levels of pJNK1 in control shRNA-treated neurons by about 30% – 40% (Fig. 5h, i). Importantly, Sema3A failed to elevate pJNK1 when TAO2 was knocked-down (Fig. 5h, i). These results indicate that TAO2 is required for Sema3A to induce pJNK1. Together, these data suggest that the interaction of TAO2 with the Sema3A-Npn1 signaling complex activates JNK1 phosphorylation to mediate neuronal differentiation in cortical pyramidal neurons.

TAO2 modulates basal dendrite formation downstream of Sema3A-Npn1

Little is known about the molecular pathways that determine the formation of basal dendrites in pyramidal neurons. Therefore, we decided to analyze whether TAO2 modulates basal dendrite formation downstream of Sema3A-Npn1. To this end, we examined whether TAO2 over-expression is sufficient to restore the defect in dendrite arborization observed in neurons from $Npn1^{Sema-}$ mice[14, 15]. These mice exhibit markedly reduced branching and growth of basal dendrites in layer V cortical neurons[14, 15]. In contrast, wild-type neurons *in situ* treated with Sema3A increase their dendritic complexity[17]. We over-expressed TAO2 in neurons dissociated from the E13.5 cortex of $Npn1^{Sema-}$ and wild-type mice. At DIV7, Sema3A treatment of $Npn1^{Sema-}$ neurons did not restore the reduced dendritic arborization complexity to wild-type levels, confirming the inability of the $Npn1^{Sema-}$ receptor to bind Sema3A (Fig. 6a, b). However, we found that TAO2 over-expression ameliorated the defective dendritic arborization in $Npn1^{Sema-}$ neurons (Fig. 6a, b). Sholl analysis of the dendritic arbors located between 10 μm and 100 μm from the cell soma revealed that dendritic arborization is restored to wildtype levels in the $Npn1^{Sema-}$/TAO2 over-expressing neurons, compared to either neurons from $Npn1^{Sema-}$ mice or $Npn1^{Sema-}$ neurons treated with Sema3A (Fig. 6b).

To further confirm the functional interaction of TAO2 and Npn1 *in vivo*, we acutely knocked down the expression of Npn1 using a shRNA construct and over-expressed TAO2 simultaneously in layer II–III cortical neurons by *in utero* electroporation. The Npn1 shRNA sequence was previously reported to down-regulate Npn1 expression in the cortex[16], and we confirmed that it efficiently knocked down the expression of Npn1-mCherry in HEK293 cells (Fig. S4a, b). E15 embryos were *in utero* electroporated with the Npn1 shRNA plasmid, or a control shRNA plasmid, together with F-GFP and rTAO2 cDNA, and sacrificed at P7. We then evaluated the dendritic morphology in neurons of the layer II-III cortex from control and Npn1 shRNA-expressing brains. The knockdown of Npn1 impaired

the formation of basal dendrites in the upper cortical layers (II-III; Fig. 6c), as had been previously reported[16]. Strikingly, TAO2 over-expression ameliorated the basal dendrite arborization deficit in Npn1 shRNA-expressing neurons (Fig. 6c). TAO2-overexpressing neurons showed a significantly increased primary basal dendrite number in neurons with Npn1 knockdown that was not significantly different from controls (Fig. 6d). However, using Sholl analysis, we found that the basal dendritic branching (secondary branching) was not restored to control levels (Fig. 6e). Importantly, Sholl analysis also demonstrated that Npn1 down-regulation did not affect the apical dendrite of transfected neurons (Fig. 6f). These results reflect a partial restoration of the formation of basal dendrites following TAO2 expression in Npn1-deficient neurons.

Our results provide evidence that Npn1 and TAO2 constitute a pathway that regulates basal dendrite development in pyramidal neurons of the developing cortex.

Activated JNK modulates basal dendrite formation downstream of TAO2

Activated JNK1 has been shown to preferentially localize to the longest neurite, presumably the axon, of cultured hippocampal neurons[31]. However, pJNK1 has also been reported to be involved in the regulation of microtubule dynamics in axons, as well as dendrites, in both hippocampus and cortex[34]. Furthermore, JNK1-deficient mice exhibit a progressive loss of microtubules within both axons and dendrites[34]. Previous to the current report, it has remained unclear whether pJNK1 modulates microtubules in basal or apical dendrites.

To assess the localization of pJNK1 in cortical pyramidal neurons, we examined its subcellular localization in DIV7 mouse cortical neurons dissociated at E17. We analyzed cells that displayed a pyramidal morphology bearing a thick “apical” dendrite and several thin “basal” dendrites. We observed that pJNK1 is enriched in developed axons (Fig. 7a) as previously reported[31]. Interestingly, we also found that the basal dendrites showed a significant increase in the intensity of pJNK1 immunoreactivity, normalized to tubulin or MAP2 immunoreactivity, compared with the apical dendrite (Fig. 7a–c). Thus, the compartmentalization of pJNK1 might play a role in the preferential elongation of basal versus apical dendrites.

To further investigate the relationship between TAO2 and JNK1 in basal dendritic arborization, we determined whether the addition of pJNK1 was able to abrogate the basal dendrite phenotypes caused by TAO2 loss-of-function. It had previously been shown that fusing MKK7 to JNK1 (MKK7-JNK1) renders JNK1 constitutively active, thus mimicking the activity of pJNK1[36, 37]. E15 mouse embryos were electroporated *in utero* with TAO2 shRNA 1 or control shRNA together with F-GFP and MKK7-JNK1 cDNA, and sacrificed at P7. TAO2 down-regulation impaired the formation of primary dendrites in layer II-III neurons (Fig. 7d, e). Interestingly, the number of primary dendrites of transfected neurons was markedly increased when MKK7-JNK1 was expressed alone or co-expressed with TAO2 shRNA1 (Fig. 7d, e). Sholl analysis demonstrated significant differences in the dendritic arborization between TAO2 shRNA 1-expressing neurons, TAO2 shRNA 1 + MKK7-JNK1-expressing neurons, and MKK7-JNK1-expressing neurons at a distance between 15 μm and 55 μm from the cell soma (Fig. 7f). However, neurons co-expressing TAO2 shRNA and MKK7-JNK1 produced basal dendrites that were not as elaborated as

those produced from control shRNA-transfected neurons (Fig. 7f). This result reflects a partial restoration of the branching of basal dendrites in TAO2 shRNA-transfected neurons following the expression of MKK7-JNK1. Importantly, MKK7-JNK1 over-expression with or without TAO2 down-regulation did not affect apical dendrite morphology compared with control-transfected neurons (Fig. 7g), further supporting a preferential basal dendrite compartmentalization of pJNK. We also found that the active JNK1 rescued the callosal axon deficit in the midline following TAO2 down-regulation (Fig. S5). Together, these experiments provide evidence that TAO2 and JNK1 modulate neuronal differentiation in cortical pyramidal neurons.

Collectively, these results delineate a molecular pathway whereby TAO2 plays a key role in governing the morphogenesis of pyramidal neurons in the developing cortex.

Discussion

In the current report, we describe a novel molecular pathway that preferentially modulates the formation of basal dendrites in cortical pyramidal neurons, and which also plays a role in axonal projection. Extensive work has addressed the roles of several molecules in dendrite arborization (for review, see [38]). However, little is known about the molecular differences that may direct the formation of different domains within the same dendritic tree. Our work represents the first approach aimed at understanding the mechanisms responsible for the delineation of basal and apical dendrites during pyramidal neuron development in the embryonic cortex.

Over a decade ago, electron microscopy studies in cultured neurons indicated that axons contain microtubules of uniform polarity, while dendrites contain microtubules of mixed polarity[39]. These data support the concept of the molecular homogeneity of the dendritic tree. However, it was recently found that apical dendrites from hippocampal CA1 and cortical layer V pyramidal neurons ubiquitously have polarized microtubule arrays[40], suggesting that the morphogenesis of dendritic subtypes (i.e. basal versus apical dendrites) may rely upon distinct cellular and molecular pathways. Accordingly, it was shown that post-Golgi membrane trafficking is polarized toward the apical dendrites of pyramidal neurons, and that the disruption of Golgi polarity produces neurons with symmetric dendritic arbors, which lack a single longest principal, or apical, dendrite[41].

The Sema3A-Npn1 signaling cascade is coupled to TAO2-JNK1 to modulate differentiation of cortical pyramidal neurons

In previous reports, activation of the Npn1 receptor by Sema3A appeared to regulate neuronal polarization[42, 43]. It was also shown that Sema3A – Npn1 signaling via PlexinA4 controls the basal dendritic arborization of cortical neurons[14–16]. Since the Npn1 receptor is likely to be uniformly distributed on all dendritic processes[15], as well as the axon[44], one question that arises is how this ubiquitous receptor specifically controls the formation of basal dendrites.

We now show that TAO2 down-regulation specifically impairs the formation of basal dendrites, without affecting apical dendrites. These data strongly suggest that TAO2 is a

mediator of the Sema3A – Npn1 pathway to sustain basal dendrite formation. Our biochemical analyses demonstrate that TAO2 and Npn1 form a complex, and that acute Npn1 down-regulation specifically impairs the formation of the basal dendrite. Importantly, we report that the deficit in basal dendrite formation following Npn1 down-regulation can be counteracted by TAO2 over-expression.

Our data also show that TAO2 appears to be uniformly distributed in the growth cones of cultured developing cortical neurons, without any preference for dendritic or axonal neurites. It is possible that our methods could not detect a differential subcellular distribution of TAO2. Alternatively, the subcellular compartmentalization of molecules that sustain basal dendrite formation may occur downstream of TAO2.

The current work implicates activated JNK1 (pJNK1) as an effector of TAO2 that modulates basal dendrite morphogenesis. It has been shown that pJNK1 is enriched in axons of hippocampal neurons in culture[31]. We also found that pJNK1 was preferentially localized to the longest neurite, presumably the axon, of DIV2 cultured cortical neurons. It has also been reported that pJNK1 is involved in the regulation of microtubule dynamics in both axons and dendrites of the hippocampus and cortex[34], and that $JNK1^{-/-}$ mice exhibit a progressive loss of microtubules within both axons and dendrites[34]. However, the role of pJNK within the different domains of the dendritic tree has not been clear. *In vivo* experiments examining the loss-of-function of the MAP kinase phosphatase 1 (MKP-1), which deactivates JNK1, show reduced dendritic arborization of cortical pyramidal neurons, as well as impaired axonal branching[35]. In agreement with these findings, we found that pJNK1 is preferentially enriched in the basal dendrites and the axons of cortical pyramidal neurons. Moreover, the over-expression of the constitutively active JNK1 counteracted defects in basal dendrite formation and axonal projection following TAO2 down-regulation. Therefore, it is plausible that the subcellular compartmentalization of pJNK1 may explain, at least in part, the specific role of TAO2 in basal dendrite formation and axonal projection (Fig. S6). Our results demonstrate that Sema3A/Npn1-mediated activation of pJNK1 requires TAO2 (Fig. 5k, l), which indicates that the three proteins act in the same pathway. Although additional independent pathways could activate JNK, the existence of such pathways does not preclude the importance of the observed TAO2-mediated activation of JNK1 in regulating dendrite morphogenesis.

TAO2 and Autism Spectrum Disorders

Autism spectrum disorder (ASD) is a heterogeneous neurodevelopmental syndrome for which there is not a clear neurobiological etiology. Although the genetic underpinnings of ASD remain elusive in most cases, a unifying model for ASD has recently been suggested[45]. This model proposes that ASD results from a developmental disconnection of brain regions that are involved in higher-order associations. Emerging literature, which shows functional and anatomical cortical under-connectivity in autistic patients, supports this model[45, 46]. The cellular basis for dysfunctional circuits, however, remains poorly understood. Several genes have been described as contributing to ASD[47–49], and it has been proposed that aberrant synaptic protein synthesis may represent one pathway leading to an autistic phenotype[50]. Recently, a novel, recurrent microdeletion, and a reciprocal microduplication, of

chromosome 16p11.2 has been identified that carries substantial susceptibility to autism and appears to account for approximately 1% of cases[7]. One of the genes from the affected region encodes for TAO2. Therefore, our findings of immature basal dendrite development and axonal projections deficits following TAO2 down-regulation support the hypothesis that underdeveloped neuron morphology contributes to the disconnection of brain regions that may underlie the autistic phenotype.

Material and Methods

shRNA and fluorescent protein constructs

The TAO2 shRNA sequences used in this study are:

TAO2 shRNA 1 = CGAGAGGACTTGAATAAGAAA;

TAO2 shRNA 2 = GCATCCTAATACCATTCAGTA.

TAO2 shRNA 3 = GTTCCAGGAGACGTGTAAGATCC.

We primarily used TAO2 shRNA 1 and 2 throughout the experiments. The TAO2 shRNA 1-resistant construct (pCMV human TAO2) is from imaGenes (Berlin, Germany), Clone: IRATp970E03140D. The sequence for the Npn1 shRNA is: AGAGAAGCCAACCATTATA[16]. The shRNAs sequences used in this study were inserted into a pSilencer vector. A pSilencer vector containing a random sequence hairpin insert was used as a control for the shRNAs. The Venus (pCAGIG) and mCherry (pCAGIG) plasmids were kindly provided by Dr. Z. Xie (Boston University). The F-GFP (pCAGIG-GAP 43-GFP) construct was gift from Dr. A. Gartner (University of Leuven, Belgium). The Myc–TAO2 (pCMV rat TAO2) was kindly provided by Dr. M. H. Cobb (University of Texas Southwestern Medical Center). The Npn1-mCherry (Plasmid 21934) and MKK7-JNK1 (Plasmid 19726) are from Addgene (Cambridge, MA).

Lentiviral production

Production of plentilox3.7 TAO2 shRNA

TAO2 shRNA was cloned into the plentilox 3.7 vector (Addgene plasmid 11795) as previously described[51]. Briefly, complimentary 5’ phosphorylated oligonucleotides FC_TAO2 sh3pllf and FC_TAO2 sh3pllr with the sequences:

tgcgagaggacttgaataagaaattcaagagatttcttattcaagtcctctcgtttttc;

tcgagaaaaaacgagaggacttgaataagaaatctcttgaatttcttattcaagtcctctcgca,

respectively, were annealed, digested with XhoI, and ligated into the plentilox 3.7 vector that had been digested with HpaI and XhoI. Proper insertion and orientation of the sequence downstream of the U6 promoter was confirmed using a sequencing primer with the sequence cagtgcaggggaaagaatagtagac.

Production and titration of virus

Lentiviral particles were made as previously described[51]. Briefly, HEK-293Tcells were plated on 10 cm dishes in 10% FBS-DMEM and transfected at 95% confluency with 8 μg

plenti 3.7, 6ug pCMV-ΔR8.9, and 5 μg pCMV-VSV-G per dish. The culture medium was switched to 30% FBS DMEM 12 hours after transfection and viral supernatant was collected 48 and 96 hours later. Viral supernatant was filtered through a 0.45μm cellular acetate vacuum filter (Corning 431155), and concentrated by ultracentrifugation at 25,000 × g for 90 minutes. Viral pellets were resuspended in DPBS+0.1% glucose and stored at −80 °C. Viral titers were determined on HEK-293T cells plated at 2×10^5 cells / well in 6-well plates, and serial dilutions of 1:200, 1:2000, and 1:20,000 were used to determine viral titer. After 48 hours of viral supernatant application, % infected cells were determined by determining % fluorescent cells/total # cells by visual inspection. Four fields of view were counted per well, and three wells were inspected per dilution. Infection was performed with MOI =10.

Antibodies

The following antibodies were used in these studies: mouse anti-acetylated tubulin (Sigma, immunocytochemistry, 1:1000), goat anti-TAO2 (K-16, Santa Cruz Biotechnology, western blot (WB) 1:2000; immunocytochemistry, 1:100), rabbit anti-pTAO2 (Ser 181; sc-135712; Santa Cruz Biotechnology; western blot (WB) 1:250; immunocytochemistry, 1:100), mouse anti-pJNK1/2 (Cell Signaling Technology, WB 1:250); rabbit anti-pJNK1/2 (Promega, immunocytochemistry, 1:200), mouse anti-pan-JNK (BD Transduction Laboratories; WB, 1:500); rabbit anti-FAK (clone C-20, Santa Cruz Biotechnology, WB, 1:500); goat anti-rat Neuropilin-1 (R&D Systems, WB, 1:500); anti-mCherry (Clontech Cat no: 632543, WB, 1:1000); anti-RFP (Abcam, ab62341, WB, 1:400); anti-actin (WB, 1:2000) and anti-GAPDH (WB, 1:500). Nuclei were visualized with Hoechst (Invitrogen) and F-actin with phalloidin (Molecular Probes). Alexa-conjugated secondary antibodies (Jackson Immunoresearch, 1:1000) were applied for 1–2 hr at 25 °C.

Cell transfection and western blot analysis

HEK293 and Ht22 cells (ATCC) were grown under standard cell culture conditions and transfected with plasmids using Lipofectamine 2000 according to the manufacturer's protocol (Invitrogen). Proteins from cell lysates were separated on 8% or 12% SDS-polyacrylamide gels at 60V and transferred onto Immobilon-P PVDF membranes (Millipore). Membranes were blocked in TBS-T (50 mM Tris-HCl pH 7.4, 150 mM NaCl, 0.1% Tween-20) with 5% non-fat dried milk for 1 h at room temperature and then incubated with primary antibody for 2 hours to overnight at 4 °C. Membranes were washed for 30 minutes in TBS-T and incubated for 1 hour at room temperature with horseradish peroxidase-conjugated secondary antibodies (GE) and then washed for 30 minutes in TBS-T. Immunoreactivity signals were detected by enhanced chemiluminescence (Perkin Elmer).

Immunoprecipitation

HEK293T cell lysates: For transient transfection, HEK293 cells were co-transfected with equal amounts of overexpression plasmids carrying myc-TAO2 and mCherry-Npn1 cDNA. The total amount of transfected DNA was between 3.5 – 4.0 μg / 35 mm plate. The cells were allowed to express the constructs for 24 h before lysis and analysis. Transfected cells were washed once with ice-cold 1X PBS and immediately lysed in 1X lysis buffer with protease inhibitors. The Bio-Rad assay kit was used to determine protein concentration. For

TAO2 and Npn1 immunoprecipitation assays, lysates were incubated with protein A sepharose conjugated to anti-mCherry antibodies overnight at 4 °C. Lysates containing 0.5 mg of protein were used for each condition. The beads were then washed with RIPA buffer twice to remove nonspecific proteins, and then washed 5 times with 1X lysis buffer before boiling in Laemmli sample buffer. Following SDS-PAGE to separate the proteins, blots were incubated with anti-TAO2 antibodies.

Cortical brain lysates: cortices from P0 Swiss Webster mice were dissected and homogenized in 350 μl of sterile-filtered 50 mM Tris-Cl pH 7.4, 120 mM NaCl, 0.5% NP-40 containing proteinase inhibitors (Roche) using a 26G-syringe, followed by a 15 min centrifugation at 14000 rpm at 4 °C and the collection of the supernatant. Following a 60 min incubation with 1–2 μg of the corresponding antibodies, 20 μl of protein G Sepharose (GE Healthcare) was added to the lysates and incubated for 45 min at 4 °C. The bound immune complexes were then collected at 8000 rpm for 3 min followed by one wash each in sterile-filtered 50 mM Tris-Cl, pH 7.4, 500 mM NaCl, 1% NP-40, and sterile-filtered 50 mM Tris-Cl pH 7.4, 120mM NaCl, 0.5% NP-40. Samples were boiled for 5 min at 95 °C, run on a 10% SDS gel and analyzed with the same primary antibodies used for the immunoprecipitation.

In utero electroporation

The Institutional Animal Care and Use Committee of Massachusetts Institute of Technology approved all experiments. Pregnant Swiss Webster mice were anesthetized by intraperitoneal injections of Ketamine 1% / Xylazine 2 mg/ml (0.01 μl/g body weight), the uterine horns were exposed, and plasmids mixed with Fast Green (Sigma) were microinjected into the lateral ventricles of embryos. The shRNA plasmid concentration was 2 to 3-fold higher than that of mCherry, Venus, or F-GFP. Five current pulses (50 ms pulse / 950 ms interval; 35–36 V) were delivered across the heads of the embryos.

Cortical cultures

Neurons were transfected by *in utero* electroporation at E15 and the transfected cortices were dissected two days later. Cortical neurons were isolated in 1X HBSS (Invitrogen) containing papain and DNase at 37 °C (Worthington). Papain was inhibited by the addition of ovomucoid (Worthington). Neurons were plated on poly-D-lysine and laminin pre-coated glass coverslips in Neurobasal / B27 medium (Invitrogen), maintained in culture for 48 h, and then fixed for immunofluorescent analysis. Neurons treated with Sema3A were dissected from brains harvested at E17 and cultured as above. Sema3A (R&D Systems) was applied 48 h later at a final concentration of 2 μg/ml. Neurons infected with lentiviral particles (infected 3hr after plating) were treated with Sema3A for 6h after 4 days in culture. Cells were either fixed as described for immunofluorescence studies, or lysed with cold RIPA buffer supplemented with phosphatase and protease inhibitors (Roche) for western blot analysis.

Immunofluorescence

Dissociated neurons: Neurons were fixed with 4% formaldehyde (FA) at 37 °C for 2 min followed by fixation for 3 min in MeOH at −20 °C. After blocking in goat serum (Zymed), neurons were incubated with the primary antibodies.

Cortical sections: Brains were removed and fixed overnight in 4% FA and thereafter transferred to 30% sucrose/PBS (4 °C, overnight). Brains were embedded in OCT compound and sectioned in a cryostat. The 20–30 μm cryosections were incubated overnight at 4 °C with the primary antibodies.

Confocal imaging

Images were taken with a Zeiss LSM 510 confocal microscope. Z-series images were collected with 1 μm steps. To perform 3D reconstructions on stacks of images of transfected cells, only Z sections in the same focal plane as GFP were used for analysis and for producing figures. 3D reconstructions and Z-stack analyses were produced using ImageJ software. The adjustment of brightness and contrast was performed on images.

Quantitative phalloidin-fluorescence determination in growth cones

Neurons were cultured for 2DIV after plating and then fixed as described above (see *immunofluorescence*). F-actin was visualized by the binding of fluorescently-labeled phalloidin. The mean intensity gray value of phalloidin in the growth cone area was measured using ImageJ.

Quantitative immunofluorescence of pTAO2, pJNK, tubulin, and MAP2 in neurites of cultured cortical neurons

Neurons were cultured for 2 DIV and 7 DIV after plating and then fixed as described (see *immunofluorescence*). pTAO2, pJNK, tubulin, and MAP2 were visualized by indirect immunofluorescence. The mean intensity gray value of a line drew along the neurites was measured using ImageJ.

Sholl analysis

All GFP-positive image stacks from transfected cortical neurons were taken as described (see *Confocal imaging*). All Sholl analyses use cortices that displayed relatively low transfection efficiencies in order to be able to select and analyze isolated transfected neurons in the cortex. Sholl analysis was performed by drawing concentric circles centered on the cell soma using Adobe Illustrator CS3. The starting radius was 15 μm and the ending radius was 55–100 μm; the interval between consecutive radii was 5 μm. All analyses were performed blindly.

Statistical analysis

Compiled data are expressed as mean ± SEM. We used the two-tailed Student's *t* test and one-way ANOVA, with posthoc Tukey or Dunnett tests, for statistical analyses. The *P* values in the Results are from *t* tests unless specified otherwise. $P<0.05$ was considered statistically significant.

Acknowledgments

We thank Dr. A. Mungenast, Dr. E. J. Kwon, Dr. M. H. Cobb, and Dr. Y Gotoh for critical reading of the manuscript, providing vectors, antibodies, and suggestions. The Simons Foundation Autism Research Initiative supported this work. †FCA is supported by a postdoctoral fellowship from the Simons Initiative on Autism and the Brain Infrastructure Grant Program. R01 MH59199 to A.L.K and D.D.G. supported this work. L.-H.T., A.L.K, and D.D.G. are investigators of the Howard Hughes Medical Institute.

References

1. Spruston N. Pyramidal neurons: dendritic structure and synaptic integration. Nat Rev Neurosci. 2008; 9:206–221. [PubMed: 18270515]
2. Mukaetova-Ladinska EB, Arnold H, Jaros E, Perry R, Perry E. Depletion of MAP2 expression and laminar cytoarchitectonic changes in dorsolateral prefrontal cortex in adult autistic individuals. Neuropathol Appl Neurobiol. 2004; 30:615–623. [PubMed: 15541002]
3. Raymond GV, Bauman ML, Kemper TL. Hippocampus in autism: a Golgi analysis. Acta Neuropathol. 1996; 91:117–119. [PubMed: 8773156]
4. Larkman AU. Dendritic morphology of pyramidal neurones of the visual cortex of the rat: III. Spine distributions. J Comp Neurol. 1991; 306:332–343. [PubMed: 1711059]
5. Chen Z, Cobb MH. Regulation of stress-responsive mitogen-activated protein (MAP) kinase pathways by TAO2. J Biol Chem. 2001; 276:16070–16075. [PubMed: 11279118]
6. Chen Z, et al. TAO (thousand-and-one amino acid) protein kinases mediate signaling from carbachol to p38 mitogen-activated protein kinase and ternary complex factors. J Biol Chem. 2003; 278:22278–22283. [PubMed: 12665513]
7. Weiss LA, et al. Association between microdeletion and microduplication at 16p11.2 and autism. N Engl J Med. 2008; 358:667–675. [PubMed: 18184952]
8. McCarthy SE, et al. Microduplications of 16p11.2 are associated with schizophrenia. Nat Genet. 2009; 41:1223–1227. [PubMed: 19855392]
9. Darnell JC, et al. FMRP stalls ribosomal translocation on mRNAs linked to synaptic function and autism. Cell. 146:247–261. [PubMed: 21784246]
10. Chen Z, Hutchison M, Cobb MH. Isolation of the protein kinase TAO2 and identification of its mitogen-activated protein kinase/extracellular signal-regulated kinase kinase binding domain. J Biol Chem. 1999; 274:28803–28807. [PubMed: 10497253]
11. Moore TM, et al. PSK, a novel STE20-like kinase derived from prostatic carcinoma that activates the c-Jun N-terminal kinase mitogen-activated protein kinase pathway and regulates actin cytoskeletal organization. J Biol Chem. 2000; 275:4311–4322. [PubMed: 10660600]
12. Yasuda S, et al. Activity-induced protocadherin arcadlin regulates dendritic spine number by triggering N-cadherin endocytosis via TAO2beta and p38 MAP kinases. Neuron. 2007; 56:456–471. [PubMed: 17988630]
13. Zihni C, et al. Prostate-derived sterile 20-like kinase 1-alpha induces apoptosis. JNK- and caspase-dependent nuclear localization is a requirement for membrane blebbing. J Biol Chem. 2007; 282:6484–6493. [PubMed: 17158878]
14. Gu C, et al. Neuropilin-1 conveys semaphorin and VEGF signaling during neural and cardiovascular development. Dev Cell. 2003; 5:45–57. [PubMed: 12852851]
15. Tran TS, et al. Secreted semaphorins control spine distribution and morphogenesis in the postnatal CNS. Nature. 2009; 462:1065–1069. [PubMed: 20010807]
16. Chen G, et al. Semaphorin-3A guides radial migration of cortical neurons during development. Nat Neurosci. 2008; 11:36–44. [PubMed: 18059265]
17. Fenstermaker V, Chen Y, Ghosh A, Yuste R. Regulation of dendritic length and branching by semaphorin 3A. J Neurobiol. 2004; 58:403–412. [PubMed: 14750152]
18. Bradke F, Dotti CG. The role of local actin instability in axon formation. Science. 1999; 283:1931–1934. [PubMed: 10082468]
19. King I, et al. Drosophila tao controls mushroom body development and ethanol-stimulated behavior through par-1. J Neurosci. 2011; 31:1139–1148. [PubMed: 21248138]

20. Barnes AP, Solecki D, Polleux F. New insights into the molecular mechanisms specifying neuronal polarity in vivo. Curr Opin Neurobiol. 2008; 18:44–52. [PubMed: 18514505]
21. Witte H, Bradke F. The role of the cytoskeleton during neuronal polarization. Curr Opin Neurobiol. 2008
22. Arimura N, Kaibuchi K. Neuronal polarity: from extracellular signals to intracellular mechanisms. Nat Rev Neurosci. 2007; 8:194–205. [PubMed: 17311006]
23. de Anda FC, Meletis K, Ge X, Rei D, Tsai LH. Centrosome motility is essential for initial axon formation in the neocortex. J Neurosci. 2010; 30:10391–10406. [PubMed: 20685982]
24. Zhou T, et al. Crystal structure of the TAO2 kinase domain: activation and specificity of a Ste20p MAP3K. Structure. 2004; 12:1891–1900. [PubMed: 15458637]
25. Romand S, Wang Y, Toledo-Rodriguez M, Markram H. Morphological development of thick-tufted layer v pyramidal cells in the rat somatosensory cortex. Front Neuroanat. 5:5. [PubMed: 21369363]
26. Polleux F, Snider W. Initiating and growing an axon. Cold Spring Harb Perspect Biol. 2010; 2:a001925. [PubMed: 20452947]
27. Huangfu WC, Omori E, Akira S, Matsumoto K, Ninomiya-Tsuji J. Osmotic stress activates the TAK1-JNK pathway while blocking TAK1-mediated NF-kappaB activation: TAO2 regulates TAK1 pathways. J Biol Chem. 2006; 281:28802–28810. [PubMed: 16893890]
28. Ben-Zvi A, et al. Semaphorin 3A and neurotrophins: a balance between apoptosis and survival signaling in embryonic DRG neurons. J Neurochem. 2006; 96:585–597. [PubMed: 16336628]
29. Tararuk T, et al. JNK1 phosphorylation of SCG10 determines microtubule dynamics and axodendritic length. J Cell Biol. 2006; 173:265–277. [PubMed: 16618812]
30. Bjorkblom B, et al. Constitutively active cytoplasmic c-Jun N-terminal kinase 1 is a dominant regulator of dendritic architecture: role of microtubule-associated protein 2 as an effector. J Neurosci. 2005; 25:6350–6361. [PubMed: 16000625]
31. Oliva AA Jr, Atkins CM, Copenagle L, Banker GA. Activated c-Jun N-terminal kinase is required for axon formation. J Neurosci. 2006; 26:9462–9470. [PubMed: 16971530]
32. Barnat M, et al. Distinct roles of c-Jun N-terminal kinase isoforms in neurite initiation and elongation during axonal regeneration. J Neurosci. 2010; 30:7804–7816. [PubMed: 20534829]
33. Rosso SB, Sussman D, Wynshaw-Boris A, Salinas PC. Wnt signaling through Dishevelled, Rac and JNK regulates dendritic development. Nat Neurosci. 2005; 8:34–42. [PubMed: 15608632]
34. Chang L, Jones Y, Ellisman MH, Goldstein LS, Karin M. JNK1 is required for maintenance of neuronal microtubules and controls phosphorylation of microtubule-associated proteins. Dev Cell. 2003; 4:521–533. [PubMed: 12689591]
35. Jeanneteau F, Deinhardt K, Miyoshi G, Bennett AM, Chao MV. The MAP kinase phosphatase MKP-1 regulates BDNF-induced axon branching. Nat Neurosci. 2010
36. Lei K, et al. The Bax subfamily of Bcl2-related proteins is essential for apoptotic signal transduction by c-Jun NH(2)-terminal kinase. Mol Cell Biol. 2002; 22:4929–4942. [PubMed: 12052897]
37. Yamasaki T, et al. Stress-activated protein kinase MKK7 regulates axon elongation in the developing cerebral cortex. J Neurosci. 2011; 31:16872–16883. [PubMed: 22090513]
38. Jan YN, Jan LY. Branching out: mechanisms of dendritic arborization. Nat Rev Neurosci. 2010; 11:316–328. [PubMed: 20404840]
39. Baas PW, Black MM, Banker GA. Changes in microtubule polarity orientation during the development of hippocampal neurons in culture. J Cell Biol. 1989; 109:3085–3094. [PubMed: 2592416]
40. Kwan AC, Dombeck DA, Webb WW. Polarized microtubule arrays in apical dendrites and axons. Proc Natl Acad Sci U S A. 2008; 105:11370–11375. [PubMed: 18682556]
41. Horton AC, et al. Polarized secretory trafficking directs cargo for asymmetric dendrite growth and morphogenesis. Neuron. 2005; 48:757–771. [PubMed: 16337914]
42. Shelly M, et al. Semaphorin3A regulates neuronal polarization by suppressing axon formation and promoting dendrite growth. Neuron. 2011; 71:433–446. [PubMed: 21835341]

43. Nishiyama M, et al. Semaphorin 3A induces CaV2.3 channel-dependent conversion of axons to dendrites. Nat Cell Biol. 2011; 13:676–685. [PubMed: 21602796]
44. Polleux F, Morrow T, Ghosh A. Semaphorin 3A is a chemoattractant for cortical apical dendrites. Nature. 2000; 404:567–573. [PubMed: 10766232]
45. Geschwind DH, Levitt P. Autism spectrum disorders: developmental disconnection syndromes. Curr Opin Neurobiol. 2007; 17:103–111. [PubMed: 17275283]
46. Just MA, Cherkassky VL, Keller TA, Kana RK, Minshew NJ. Functional and anatomical cortical underconnectivity in autism: evidence from an FMRI study of an executive function task and corpus callosum morphometry. Cereb Cortex. 2007; 17:951–961. [PubMed: 16772313]
47. Walsh CA, Morrow EM, Rubenstein JL. Autism and brain development. Cell. 2008; 135:396–400. [PubMed: 18984148]
48. Weiss LA, Arking DE, Daly MJ, Chakravarti A. A genome-wide linkage and association scan reveals novel loci for autism. Nature. 2009; 461:802–808. [PubMed: 19812673]
49. Pinto D, et al. Functional impact of global rare copy number variation in autism spectrum disorders. Nature. 2010; 466:368–372. [PubMed: 20531469]
50. Kelleher RJ 3rd, Bear MF. The autistic neuron: troubled translation? Cell. 2008; 135:401–406. [PubMed: 18984149]
51. Mao Y, et al. Disrupted in schizophrenia 1 regulates neuronal progenitor proliferation via modulation of GSK3beta/beta-catenin signaling. Cell. 2009; 136:1017–1031. [PubMed: 19303846]

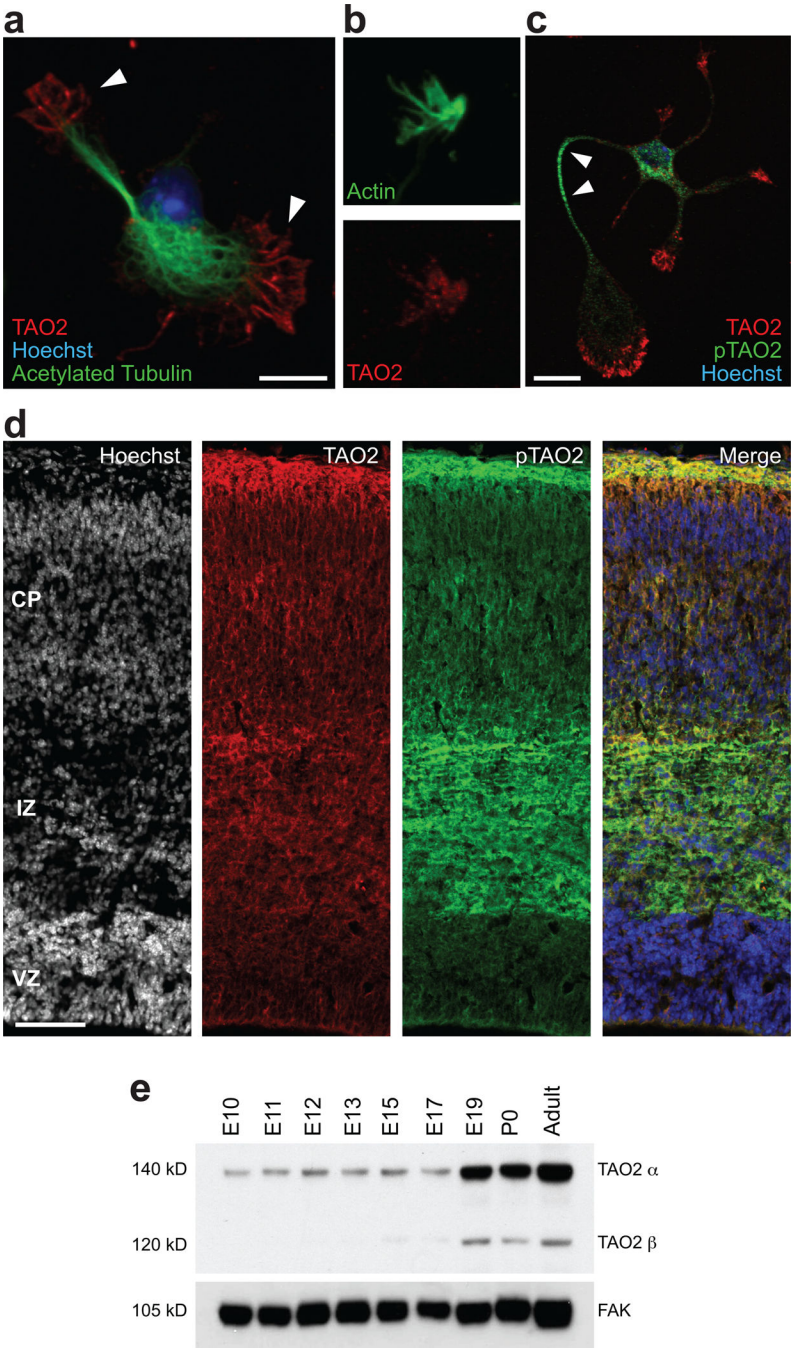

Figure 1. Distribution of TAO2 and activated TAO2 in cultured neurons and the developing cerebral cortex

(**a**) TAO2 localizes to the growth cones (white arrowheads) of isolated cortical neurons. (**b**) TAO2 (red) co-localizes with actin (green) in growth cones. (**c**) Activated TAO2 (pTAO2; green) localizes to the neurite shaft of isolated cortical neurons. (**d**) TAO2 and pTAO2 are preferentially expressed in the IZ and CP of the developing cortex. (**e**) Western blotting reveals that TAO2α expression levels are constant during early cortical embryonic

development, but increase considerably at perinatal (E19, P0) and adult time points. The TAO2β isoform is absent prior to E19. Scale bar: 10 μm (a), 200 μm (c).

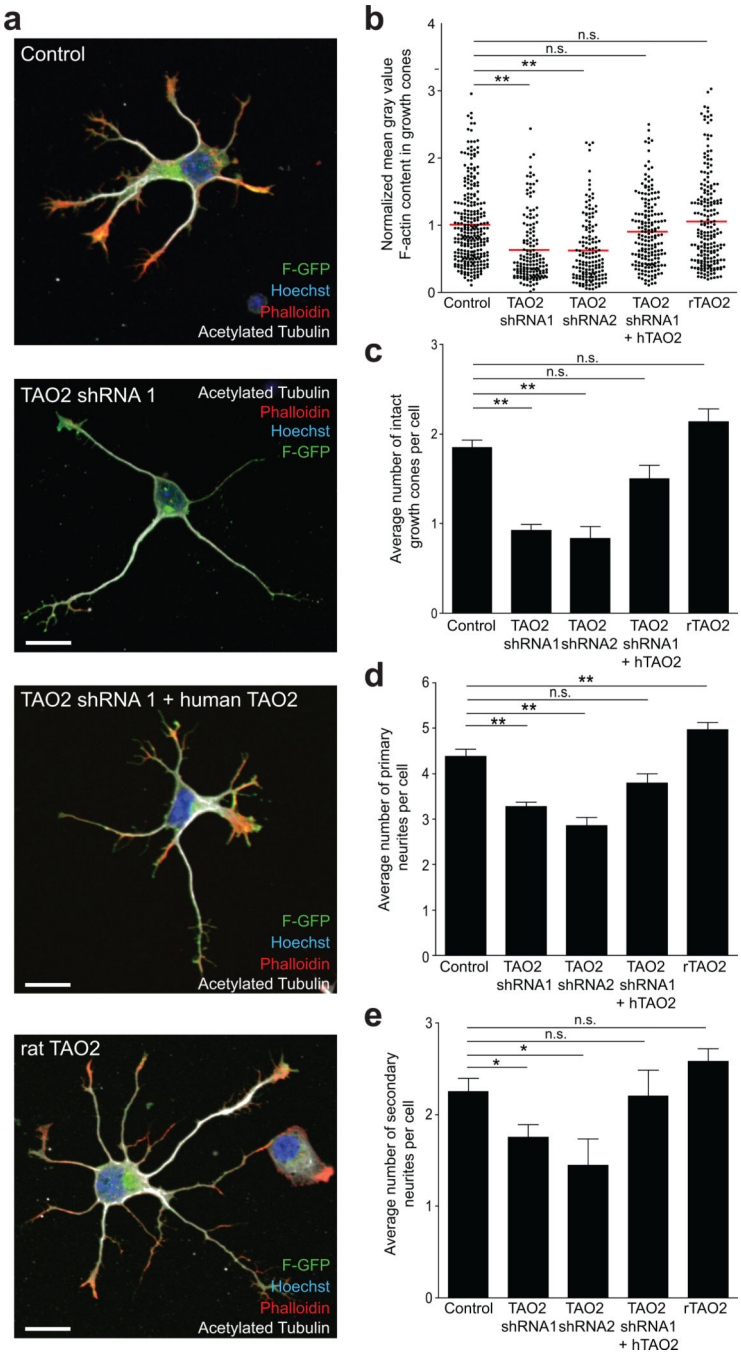

Figure 2. TAO2 down-regulation or over-expression affects the differentiation of isolated cortical neurons

(**a**) TAO2 down-regulation and over-expression have opposite effects in the complexity of cortical neurons. TAO2 shRNA-transfected neurons display fewer branched neurites, with collapsed growth cones. Expression of an shRNA-resistant human TAO2 cDNA (hTAO2) counteracts TAO2 down-regulation. Rat (r)TAO2 over-expression increases neuronal complexity with more primary neurites. (**b**) Quantification of F-actin content in growth cones. TAO2 silencing decreased the levels of F-actin in growth cones (control: n=44 cells/

three cultures; TAO2 shRNA 1: n=43 cells/three cultures; TAO2 shRNA 2: n=36 cells/two cultures; $P<0.0001$ by one-way ANOVA, posthoc Dunnett test $^{**}P<0.01$). (**c**) Quantification of the number of intact (non-collapsed) growth cones per transfected cell. TAO2 silencing decreased the number of intact growth cones per cell (control: n=160 cells/three cultures; TAO2 shRNA 1: n=133 cells /three cultures; TAO2 shRNA 2: n=36 cells/two cultures; $P<0.0001$ by one-way ANOVA, posthoc Dunnett test $^{**}P<0.01$). (**d, e**) TAO2 down-regulation decreases the number of primary (control: n=168 cells/three cultures; TAO2 shRNA 1: n=149 cells/three cultures; TAO2 shRNA 2: n=36 cells/two cultures; $P<0.0001$ by one-way ANOVA, posthoc Dunnett test $^{**}P<0.01$) and secondary neurites ($P=0.0102$ by one-way ANOVA, posthoc Dunnett test $^{*}P<0.05$) per transfected cell. TAO2 over-expression increases the number of primary neurites (rTAO2: n=119 cells/three cultures; $P<0.0001$ by one-way ANOVA, posthoc Dunnett test $^{**}P<0.01$). Mean ± s.e.m. Scale bar: 10 μm.

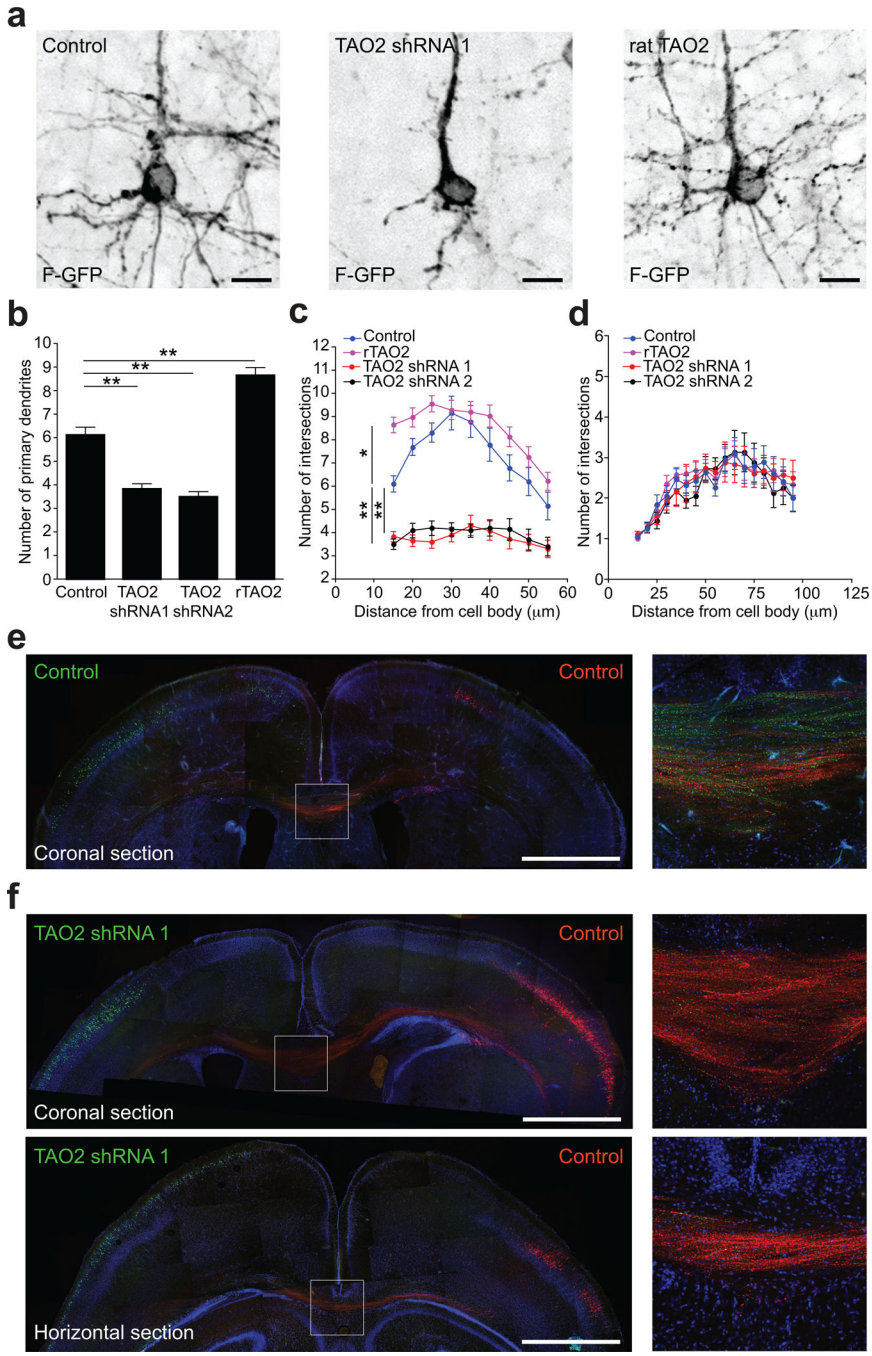

Figure 3. TAO2 down-regulation or over-expression affects basal dendrite arborization and callosal axon projection in the developing cortex

(**a**) TAO2 knockdown or up-regulation have opposite effects in basal dendrite development *in vivo*. (**b**) The number of primary dendrites decreases following TAO2 knockdown and increases following rTAO2 over-expression (control: n=19 cells/three brains; TAO2 shRNA 1: n=23 cells/three brains; TAO2 shRNA 2: n=20 cells/two brains; rTAO2: n=31 cells/three brains; $P<0.0001$ by one-way ANOVA, posthoc Dunnett test $^{**}P<0.01$). (**c**) Sholl analysis of the dendritic arbor from upper cortical layer transfected neurons ($P<0.0001$ by one-way

ANOVA, posthoc Dunnett test $^{**}P < 0.01$, $^{*}P < 0.05$). (**d**) Sholl analysis of apical dendrites from cells in (c). (**e, f**) TAO2 shRNA-mediated down-regulation diminishes the number of callosal axons traversing the midline (n=3 brains per condition). (**e**) Control transfected neurons in both hemispheres (Venus: left hemisphere; mCherry: right hemisphere) project callosal axons that crossed the midline. Right panel: inset of the corpus callosum. (**f**) TAO2 knock-down in Venus-positive neurons prevents axons from these cells from crossing the midline. Upper panel: coronal brain section. Lower panel: horizontal brain section. Right panels: inset of the corpus callosum from the coronal (upper panel) and horizontal section (lower panel). Mean ± s.e.m. Scale bar: 10 μm (a) and 500 μm (e, f).

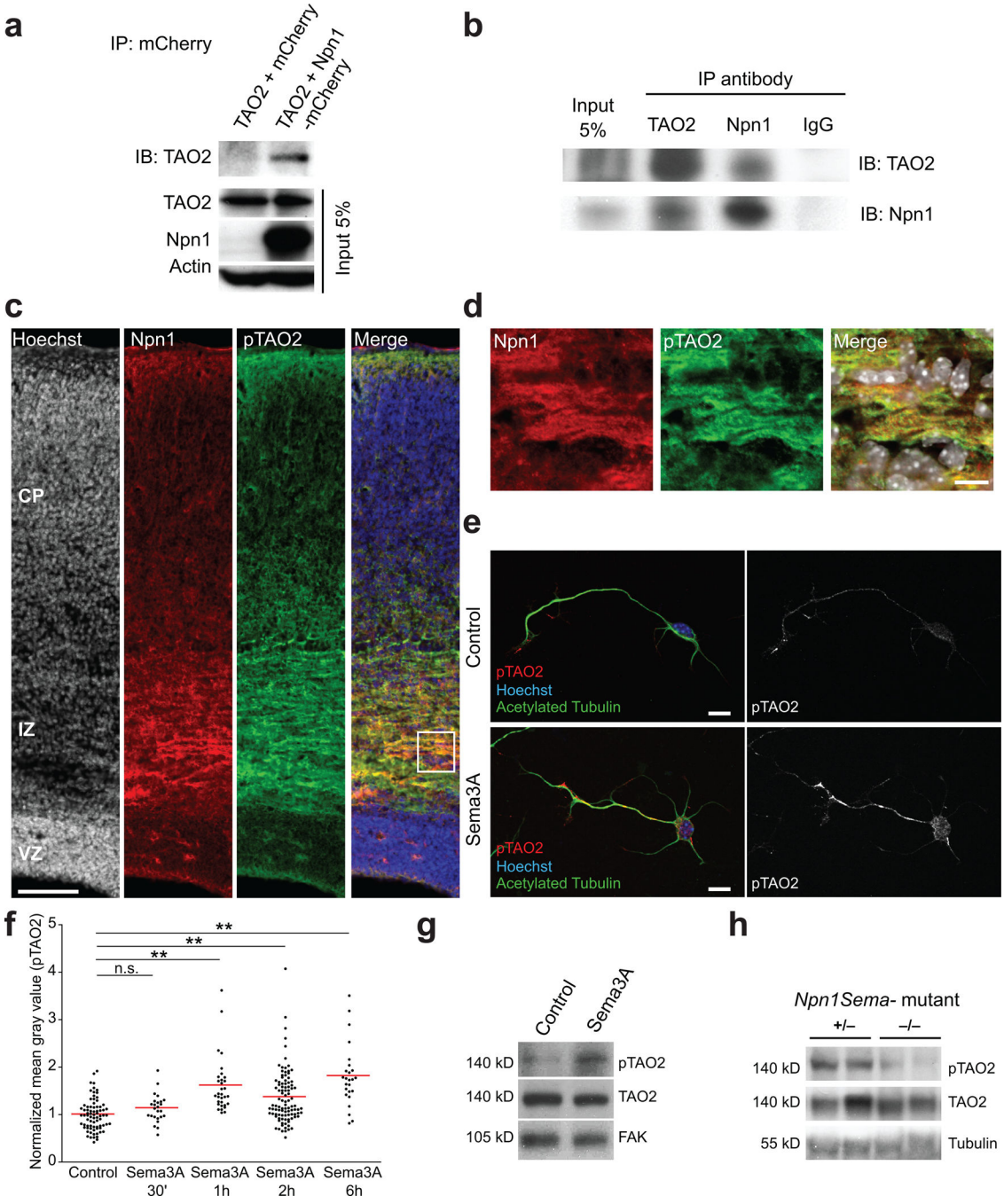

Figure 4. TAO2 interacts with Npn1 to modulate TAO2 phosphorylation

(**a**) Immunoprecipitation with anti-mCherry antibodies demonstrates the interaction of Npn1 and TAO2. HEK293T cells were transfected with Npn1-mCherry and Myc-TAO2. The input lane represents 5% of the total protein quantity used for immunoprecipitation. (**b**) TAO2 co-immunoprecipitates with Npn1 in the developing cortex. The input lane represents 5% of the total protein quantity used for immunoprecipitation. (**c**) Npn1 and pTAO2 are preferentially expressed in the IZ and CP of the developing cortex. (**d**) Inset from (c), white box: Npn1 and pTAO2 co-localize in the developing cortex. (**e–g**) Sema3A treatment (2

μg/ml) increases pTAO2 immunoreactivity in cultured cortical neurons. (**e**) Control neuron (upper panel) and a neuron treated with Sema3A for 2h (lower panel) (**f**) Quantification of pTAO2 immunoreactivity from the longest neurite of control and Sema3A-treated cultured cortical neurons (control: n=77 cells/three cultures, Sema3A 30 min: n=25 cells/two cultures, Sema3A 1h: n=32 cells/three cultures, Sema3A 2h: n=99 cells/three cultures, Sema3A 6h: n= 25 cells/three cultures; $P<0.0001$ by one-way ANOVA, posthoc Dunnett test $^{**}P<0.01$). (**g**) Immunoblot of cultured cortical neuron lysates shows that the 2h Sema3A treatment increases pTAO2 immunoreactivity. (**h**) Immunoblot of cortical lysates from $Npn1^{Sema-}$ heterozygous (+/−) and $Npn1^{Sema-}$ homozygous (−/−) P7 mice littermates shows a decrease in pTAO2 immunoreactivity in the −/− mouse compared with the +/− littermate. FAK and tubulin are used as the loading controls. Scale bar: 500 μm (c) and 10 μm (d, e).

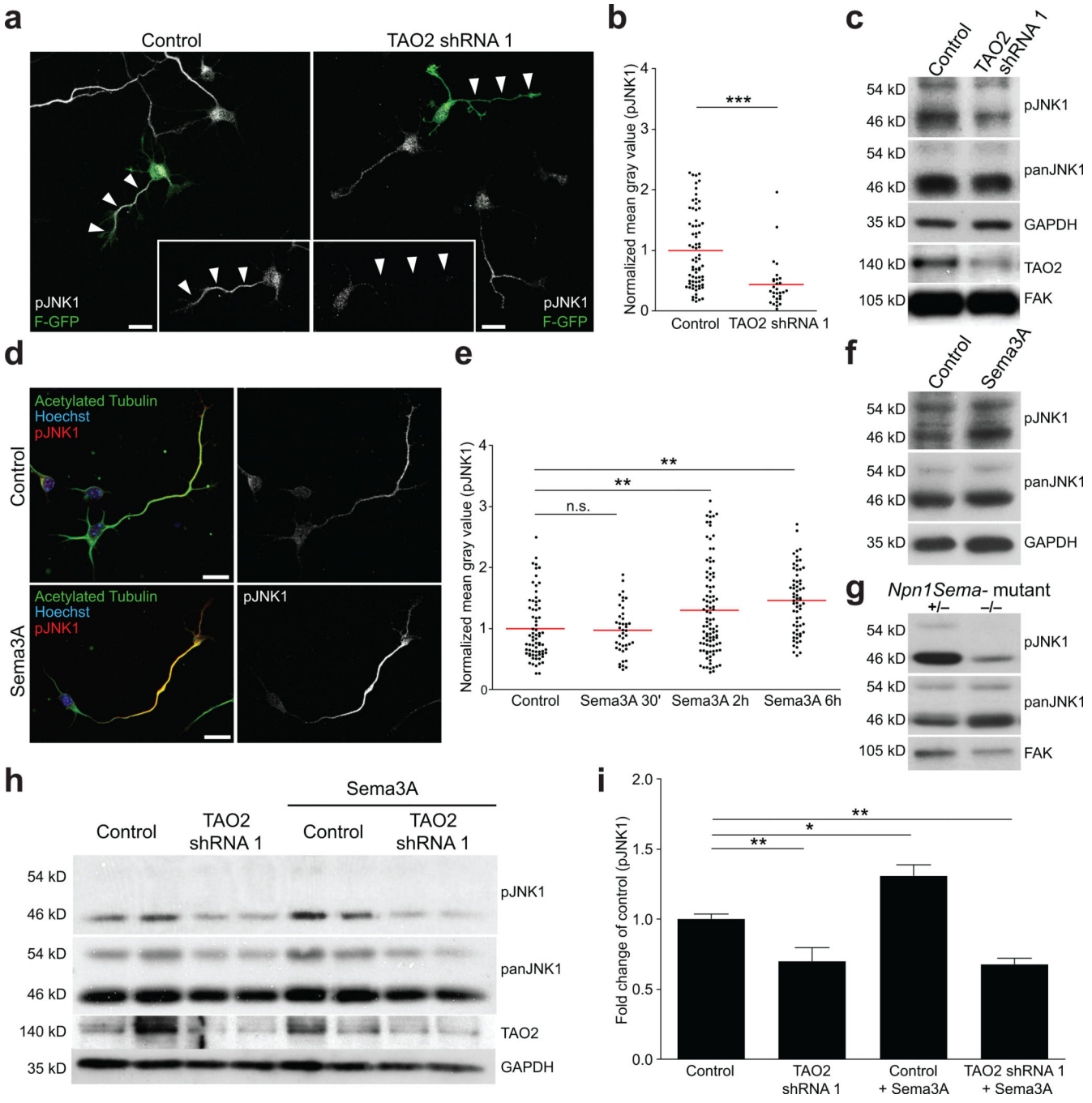

Figure 5. TAO2 and Sema3A modulate the activity of JNK1

(**a**) TAO2 down-regulation decreases pJNK1 immunoreactivity in cortical neurons (right panel, white arrowheads) compared to control neurons (left panel, white arrowheads). (**b**) Quantification of pJNK1 immunoreactivity in the longest neurite of control and TAO2 down-regulated cortical neurons (control: n=72 cells/two cultures; TAO2 shRNA 1: n=29 cells/two cultures; ***P<0.0001 by t test). (**c**) TAO2 down-regulation decreases JNK1 phosphorylation (46 kD) in Ht22 cells. (**d–f**) Sema3A treatment (2 μg/ml) increases pJNK1 immunoreactivity in cortical neurons. (**d**) Control neuron (upper panel) and a neuron treated

with Sema3A for 2h (lower panel). (**e**) Quantification of pJNK1 immunoreactivity from the longest neurite of control and Sema3A-treated cortical neurons (control: n=71 cells/three cultures, Sema3A 30 min: n=42 cells/two cultures, Sema3A 2h: n=97 cells/three cultures, Sema3A 6h: n= 64 cells/three cultures; $P<0.0001$ by one-way ANOVA, posthoc Dunnett test $^{**}P<0.01$). (**f**) Immunoblot of cultured cortical neuron lysates shows that Sema3A 6h treatment increases pJNK1 immunoreactivity (46 kD) compared to control. (**g**) Immunoblot of cortex lysates from *Npn1*$^{Sema-}$ +/− and −/− P7 littermate mice shows a decrease in pJNK1 immunoreactivity (46 kD) in the −/− mouse compared with the +/− littermate. (**h**) Western blotting reveals that isolated cortical neurons infected with TAO2 shRNA 1 lentivirus failed to increase levels of pJNK1 in the presence of Sema3A 6h. (**i**) Quantification of pJNK1 (46 kD) immunoreactivity from (h) (n=2 experiments per triplicate; $P<0.0001$ by one-way ANOVA, posthoc Dunnett test $^{**}P<0.01$, $^{*}P<0.05$). FAK and GADPH are used as the loading controls. Mean ± s.e.m. Scale bar: 10 μm.

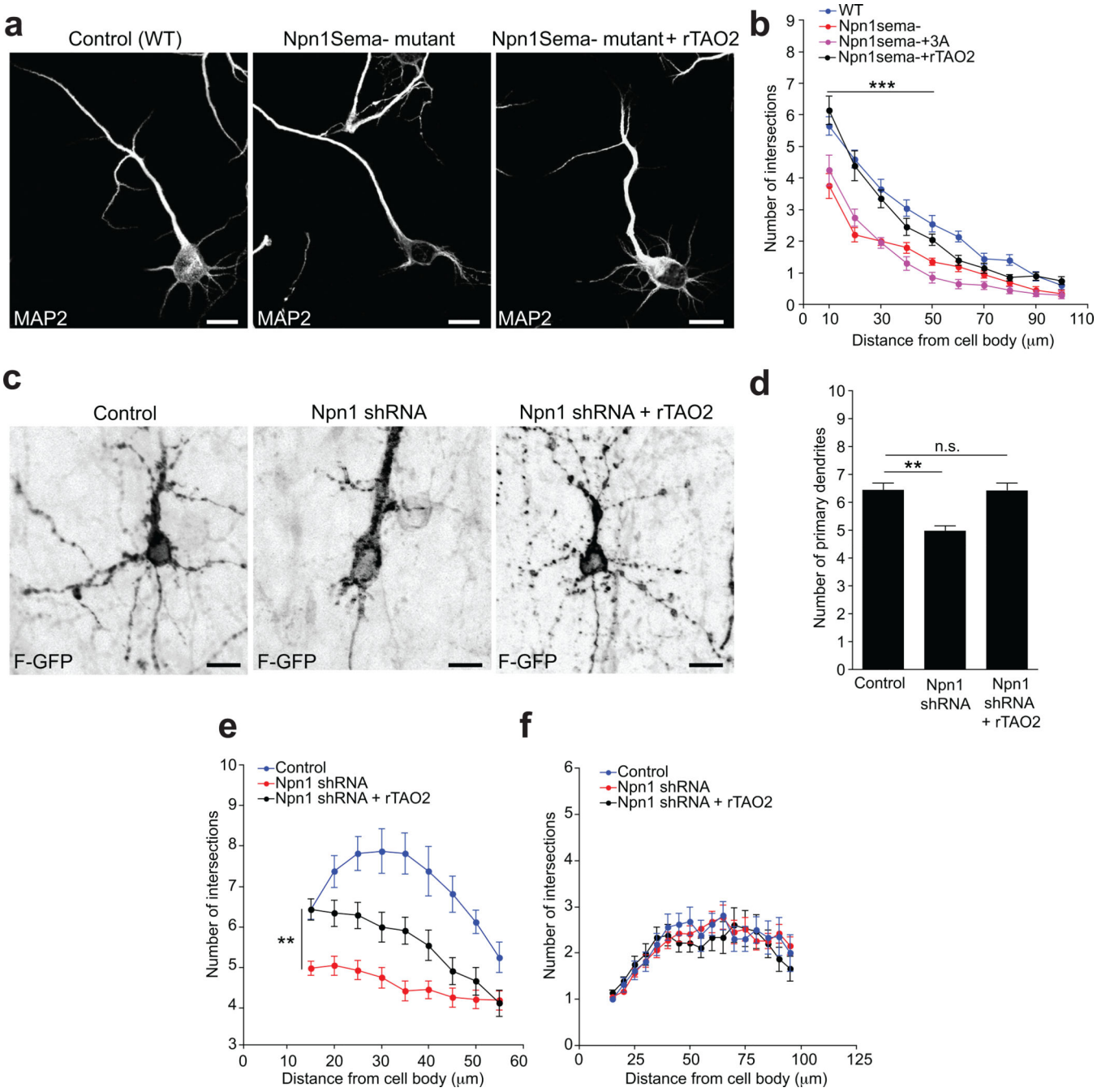

Figure 6. TAO2 counteracts the dendritic arborization deficit in neurons expressing a deficient Npn1 receptor or with Npn1 down-regulation

(**a**) rTAO2 over-expression ameliorates the dendritic arborization deficit in primary cortical *Npn1*$^{Sema-}$ neurons. (**b**) Sholl analysis of the dendritic arbors reveals no statistical differences between wildtype (WT) and *Npn1*$^{Sema-}$ + rTAO2 over-expressing cultured neurons at a distance between 10 μm and 100 μm from the cell soma (n=20 cells per condition/two cultures, ***P<0.001 by t test). (**c**) rTAO2 over-expression reverses the basal dendritic arborization deficit in Npn1 shRNA-transfected neurons from II–III layer cortex. (**d**) rTAO2 over-expression restores the number of primary dendrites in Npn1 down-

regulated neurons (control: n=16 cells/two brains; Npn1 shRNA: n=47 cells/ three brains; Npn1 shRNA + rTAO2: n=35 cells/three brains; $P<0.0001$, by one-way ANOVA, posthoc Dunnett test $^{**}P<0.01$). (**e**) Sholl analysis of the dendritic arbors shows significant differences between Npn1 shRNA-expressing neurons and Npn1 shRNA + rTAO2-expressing neurons ($P<0.0001$ by one-way ANOVA, posthoc Dunnett test $^{**}P<0.01$). (**f**) Sholl analysis of the apical dendrite does not show any differences between Npn1 down-regulation, Npn1 shRNA + rTAO2 over-expression, and control conditions. Mean ± s.e.m. Scale bar: 10 μm.

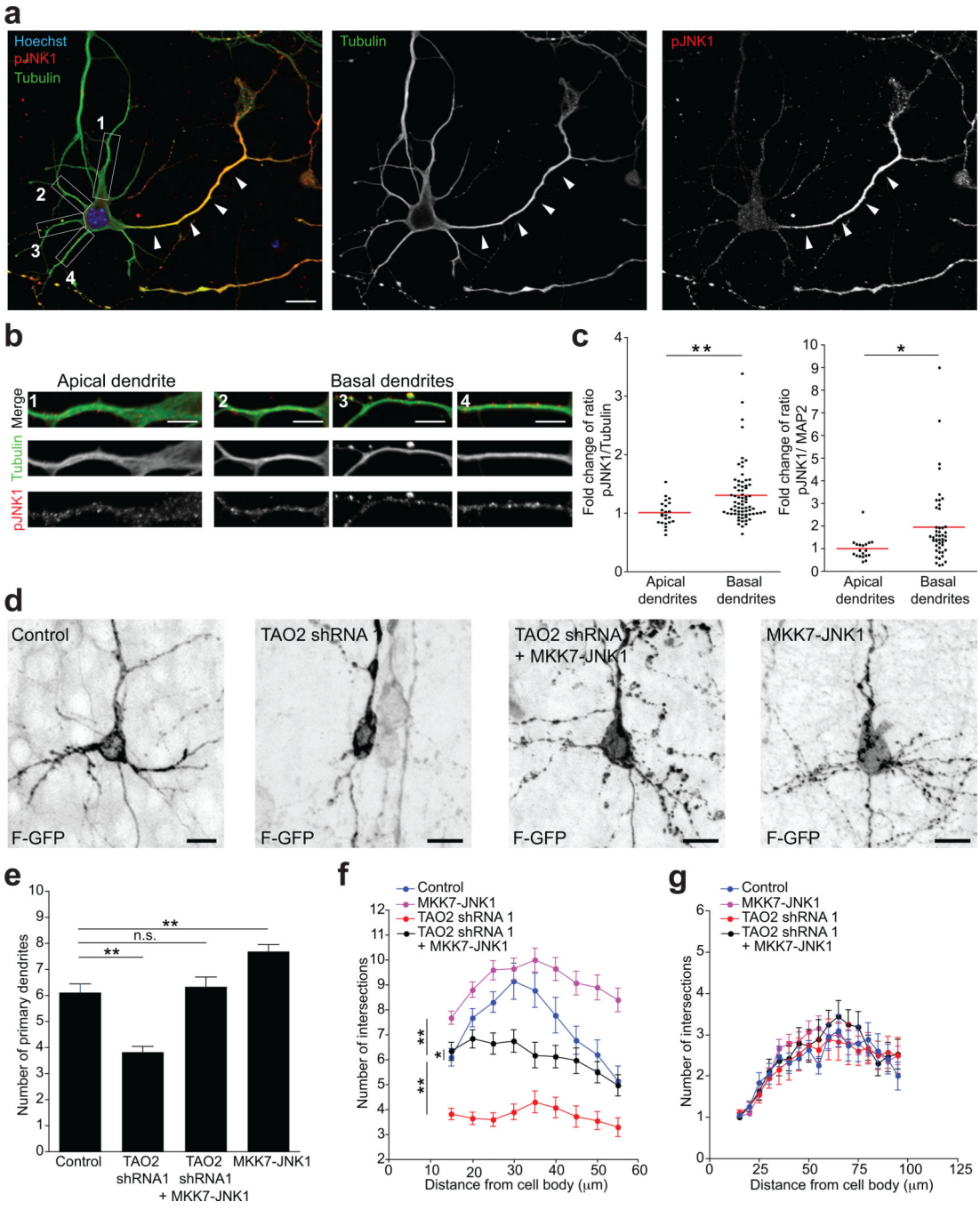

Figure 7. Activated JNK1 ameliorates deficient basal dendrite formation following TAO2 down-regulation

(**a**) Cultured cortical pyramidal neuron immunolabeled for tubulin (green) and pJNK1 (red). Activated JNK1 is enriched in the axon (white arrowheads). (**b**) The insets show the apical dendrite (1) and basal dendrites (2, 3, 4) from the cell in (a). (**c**) The quantification of the ratio of pJNK1 and tubulin or MAP2 fluorescence intensities shows a higher ratio of pJNK1/ tubulin and pJNK1/MAP2 in basal dendrites compared with apical dendrites. Values are normalized to the mean of apical dendrites (tubulin: n=23 cells/three cultures; MAP2: n=20

cells/three cultures; **P=0.0051, *P=0.0154 by t test;). (**d**) Upper cortical layer (II–III) transfected neurons show underdeveloped basal dendrites following shRNA-mediated knockdown of TAO2 compared with control-transfected neurons. MKK7-JNK1 over-expression ameliorates the basal dendrite deficit following TAO2 shRNA-mediated down-regulation. MKK7-JNK1 over-expression alone increases the number of basal dendrites compare with control-transfected cells. (**e**) The number of primary dendrites increases following MKK7-JNK1 over-expression (control: n=19 cells/three brains; TAO2 shRNA 1: n=23 cells/three brains; TAO2 shRNA 1 + MKK7-JNK1: n=32 cells/three brains; MKK7-JNK1: n=42 cells/three brains; ***P<0.0001 by one-way ANOVA, posthoc Dunnett test **P<0.01). (**f**) Sholl analysis of the dendritic arbor from upper cortical layer transfected neurons (***P<0.0001 by one-way ANOVA, posthoc Dunnett test **P<0.01, *P<0.05). (**g**) Sholl analysis of apical dendrites from cells in (f). Quantifications for control and TAO2 shRNA 1-transfected cells are the same as in Figure 3b–d. Mean ± s.e.m. Scale bar: 10 μm (a) and 5 μm (b).